

PACS 77.84.Bw, 82.80.Gk

## **Biomorphic SiC from peas and beans**

**V.S. Kiselov, V.A. Yukhymchyk, V.I. Poludin, M.P. Tryus, A.E. Belyaev**

V. Lashkaryov Institute of Semiconductor Physics, NAS of Ukraine,

41, prospect Nauky, 03028 Kyiv, Ukraine

*E-mail: vit\_kiselov@ukr.net*

**Abstract.** Biomorphic porous SiC ceramics produced by impregnation with liquid or vapor silicon of carbon matrices derived from peas (*Pisum sativum L.*) and beans (*Phaseolus*) precursors were investigated. Optical and scanning electron microscopy was used to study the structure of ceramics. It was shown that SiC ceramics made from endosperm of peas and beans seeds has inherited the alveolate structure and possesses many hierarchical pores with diameters varying between 20 to 100  $\mu\text{m}$ . Raman spectroscopy investigations showed that the 3C polytype is formed at a synthesis temperature of about 1550  $^{\circ}\text{C}$ , and that both 3C and 6H-SiC are formed at temperatures of about 1800  $^{\circ}\text{C}$ . It is shown possibilities of production of ceramic articles of various forms from seeds.

**Keywords:** biomorphic SiC ceramics, Raman scattering, SEM.

Manuscript received 03.07.12; revised version received 26.09.12; accepted for publication 17.10.12; published online 12.12.12.

### **1. Introduction**

In the recent decade, great efforts were devoted to the development of different kinds of biotechnologies, which is caused by a wide spectrum of problems in medicine, pharmacology and industry. One of the ways of preparation of new porous biomaterials is the method of biotemplating. It used different biological objects for synthesis of new porous materials. These materials are pseudomorphic to the initial biological objects on the micro-, meso-, and macroscales. Biotemplating is a relatively new way of production of ceramic materials with a complicated porous structure. This alternative technique is very simple and cost-effective as compared to traditional lithography that is widely used in microelectronics. Cellular structures available in nature are particularly interesting as natural replica templates, mainly due to their specific pore morphology and intricate microstructures, which might be difficult to produce artificially. Materials containing predetermined porosity exhibit special properties and features. They are interesting due to their particular properties such as low density, low thermal conductivity, thermal stability, high-surface area, and high permeability. Nowadays, except for medicine, such porous materials find many

applications as filters, diesel particulate filters, catalyst and membrane supports. There are known works on using millet [1], egg shell membrane, butterfly wings and sea urchin [2-4], marine algae and plants [5] for producing biomorphic SiC materials. Following the same biomimetic approach, many investigators have studied the transformation of wood cellular structures into macro porous ceramics [6–11].

In this work, we obtain and investigate porous SiC ceramics prepared from the family of leguminous cultures – peas and beans.

### **2. Experimental details**

#### *2.1. The first step. Production and investigation of carbon matrix*

In our investigations, we used seeds of dicotyledonous (*Licotyledoneae*) metperm plants – peas (*Pisum sativum L.*) and beans (*Phaseolus*). Preparation of biomorphic SiC includes two steps. First, a carbon template is prepared using the pyrolysis of natural specimens in inert atmosphere. The specimens were heated for 6-8 h in a horizontal silica pipe furnace in argon flow ( $\square 10 \text{ cm}^3/\text{min}$ ). To avoid the collapse of the specimen structure, it was slowly heated up to 400  $^{\circ}\text{C}$  with the rate

1-2 °C/min. Subsequently, the temperature was increased up to 900 °C with the rate 5-6 °C/min to obtain a porous carbon template. In some special cases, we realize pyrolysis up to 2000 °C. During the pyrolysis, H<sub>2</sub>O, CO<sub>2</sub>, acids, carbonyl groups and alcohols are released due to decomposition of biopolymer structures at temperatures above 600 °C. Meanwhile, the major biopolymer constituents of cell wall materials are rearranged and converted into carbon struts.

Under pyrolysis at the initial stage ( $T \leq 400$  °C), the seeds of peas, beans, millets and wheat are increased in their sizes. Subsequent growth of the temperature leads to shrinkage up to 20-25%. Therefore, we carry out this operation by two ways: in closed volume and in open volume. In the first way, we obtained a cemented carbon matrix having the form of closed volume used under pyrolysis. In the second way, we produced a carbon matrix from individual seeds. The unique anatomical features of the native beans tissue can be retained during pyrolysis, which yields a porous template composed primarily of carbon.

Peas and beans define the presence of two separate cotyledons. In Fig. 1a, the structure of the seeds is shown. It consists of endosperm (1), embryo (2), seed coat (3) and inner shells (4). The SEM images of the surfaces of seed coat and inner shells are shown in Fig. 1b. To investigate the inner microstructure of the carbon template, a complete carbon matrix was split across in three cross directions A-A, B-B and C-C. Fig. 2a shows the SEM images of the cross section of bean. From these images, it can be seen that the carbon template has indeed inherited the alveolate structure of endosperm and possesses many hierarchical pores with diameters varying between 20 to 100 μm. These pores are almost uniformly distributed. The size of pores in matrix increases with sizes of the initial seeds.

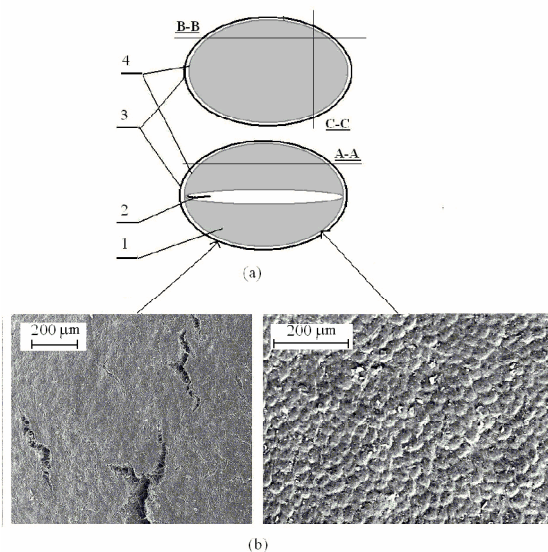


**Fig. 1.** The structure of the carbon matrix made from seeds of dicotyledonous (*Licotyledoneae*) metperm plants (a) and the photo of the surface of seed coats and inner shells (b).

## 2.2. The second step.

### Impregnation by Si and synthesis of SiC

At the second step, the carbon template is transformed into bio-SiC by impregnation with Si and subsequent synthesis of SiC. For impregnation, we removed seed coats and inner coats from the seeds. The REDMET-30 industrial furnace was used for thermal operations. Carbon matrix and silicon were added to individual crucibles from tight graphite. Impregnation was realized under a variable pressure of He within the temperature range  $T = 1600-1900$  °C and duration  $t_s = 10-30$  min. At high temperatures, liquid or vapor silicon spontaneously infiltrated into the carbon template and produced SiC ceramics. It should be noted that due to small sizes and irregular shape of specimens, it was difficult to provide impregnation only with liquid or vapor silicon. In certain cases on the surface of ceramics we can observe areas obtained by impregnation with liquid and vapor silicon.

Biomorphic SiC ceramics depending on the impregnation method with liquid or vapor silicon can be crystalline or amorphous. As a rule, the ceramics prepared using impregnation with liquid silicon consists of SiC faceted microcrystals with the size 4–5 μm, Fig. 3a. It was ascertained that the mechanical properties, structure and color of biomorphic SiC depend on the carbon template infiltration method [12]. Melt impregnation resulted in final material with high mechanical strength and green-brown color, while impregnation with Si vapor resulted in final material of white color with amorphous structure, Fig. 3b. If required, excess carbon in final products was burn out in the furnace in oxygen atmosphere at  $T = 900$  °C for 2 h.

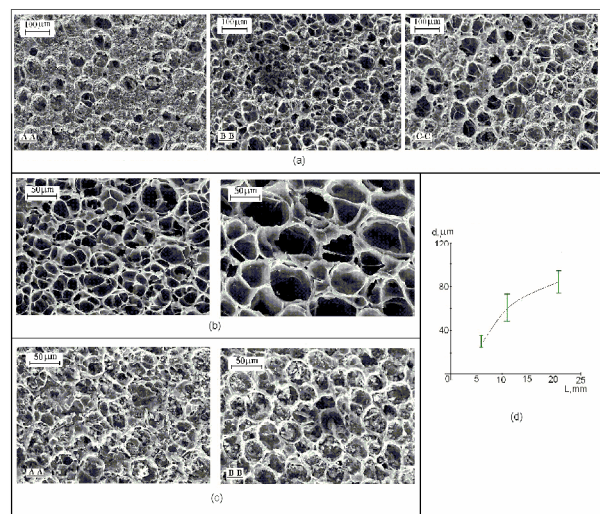


**Fig. 2.** The surface SEM image of the carbon matrix from beans ((a), (b)), peas (c). Dependence of pore size  $d$  on longitudinal sizes of carbon matrices (d).

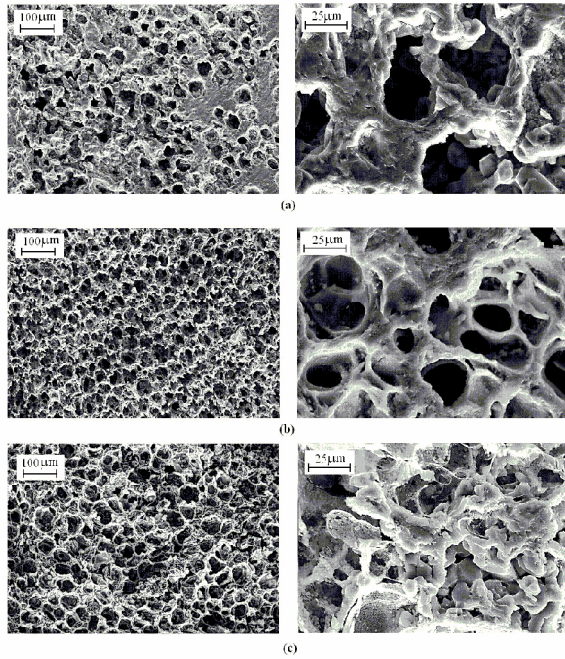


**Fig. 3.** SEM image of surface of the biomorphic SiC ceramics: (a) peas, impregnation with liquid silicon, (b) peas, impregnation with vapor silicon, and (c) beans, impregnation with vapor silicon.

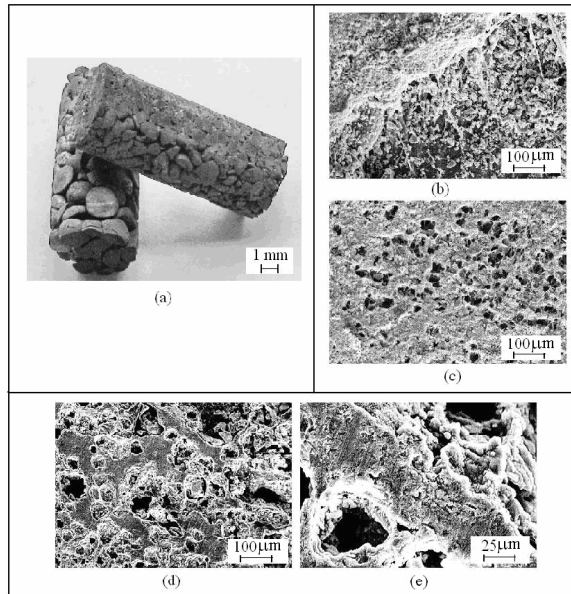


**Fig. 4.** Typical ceramic samples obtained by pyrolysis in closed volume and subsequent impregnation with liquid silicon (a); SEM image of surface of the biomorphic SiC ceramics from parts of *Agaricus*: underside of cap (*pileus*) (b), plates from stipe (c), and that from potato plates ((d), (f)).

In Fig. 4a, it is shown the ceramic sample obtained by pyrolysis in closed volume and subsequent impregnation with liquid silicon. So, this process opens possibilities for production of ceramic articles with various forms. In addition, it must be noted that by this

method biomorphic SiC materials can be obtained from many foodstuffs. In particular, we produce such porous ceramics from parts of common mushroom (*Agaricus*) (Figs. 4b and 4c) and potato plates (Figs. 4d and 4e).

### 3. Results and discussion

The structure and composition of the materials obtained were investigated by Raman spectroscopy. Fig. 5 shows Raman spectra of the carbon matrix that was obtained directly after pyrolysis (curve 1) and after additional high-temperature annealing (curves 2 and 3). The quantitative characterization of the structural imperfection of graphite by using Raman spectroscopy was first done in the work [13]. The authors [13] suggested estimating the value of the correlation length  $L_a$  in the plane of the graphite sheet (in other words – the areal size of the graphite cluster) based on the intensity ratio typical for  $D$  and  $G$  bands:

$$\frac{I(D)}{I(G)} = \frac{C(\lambda)}{L_a}, \quad (1)$$

where  $C(\lambda) = 4.4 \text{ nm}$  for  $\lambda = 514.5 \text{ nm}$ . After deconvolution of the experimental Raman bands by components and calculation of their integrated intensity, we obtained the  $L_a$  based on Eq. (1) equal to 1.5 and 4.1 nm for spectra 2 and 3, respectively. This analysis shows, therefore, that the minimum size of the graphite clusters increased after the thermal treatment. Note that Eq. (1) is valid for the quantitative estimation of a confined  $sp^2$  structure only when its imperfection is related with confinement in the graphite sheet plane. Moreover, it was assumed in [13] that the graphite nanocrystallites are monomodal with respect to the  $L_a$ -dimension. At the same time, for an ensemble of crystallites with the size distribution, in which the portion of nanocrystallites with size  $L_{ai}$  comprises the  $X_i$  part of the cluster, the effective value of  $L_{a,eff}$  is given by [14]:

$$\frac{1}{L_{a,eff}} = \sum_i^N X_i \frac{1}{L_{ai}}. \quad (2)$$

In this case, the correlation length calculated in accord with Eq. (1) is dominated by the smallest  $L_{ai}$ . As to other kinds of distortion of the graphite spatial symmetry (for example due to a high concentration of impurities), for each of them  $C(\lambda)$  in (1) will be different.

In addition to the intensity ratio of  $D$  and  $G$  bands, a degree of disorder is frequently estimated from their frequency shifts and bandwidths (full width at half maximum, FWHM). For the structures under study here, the FWHM decreases after annealing, indicating the reduced concentration of defects in carbon matrix. Note that since during the synthesis of bio-SiC, the carbon matrices formed by pyrolysis are kept for a certain time within the given temperature range (1450-2000 °C), they were not additionally annealed.

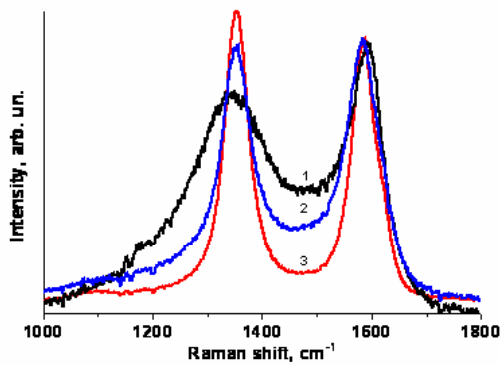


Fig. 5. Raman spectra of carbon template after pyrolysis at 900 °C (1) and after additional high-temperature annealing (2, 3).

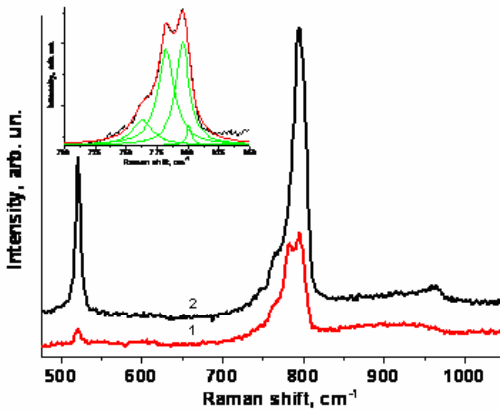


Fig. 6. Raman spectra of bio-SiC ceramics produced by impregnation with gaseous silicon (1) and liquid silicon (2). The inset shows deconvolution of TO bands in spectra of 6H and 3C polytypes by separate Lorentz components.

In Fig. 6, the Raman spectra of formed SiC ceramics are shown. Curves 1 and 2 correspond to the SiC structures formed by impregnation of carbon matrix with gaseous and liquid silicon, respectively. It can be concluded from observation of the transversal optical mode of SiC ( $\omega_{\text{TO}} = 796 \text{ cm}^{-1}$ ) that silicon carbide was formed in both cases. In addition, the band related with Si–Si vibrations,  $\omega_{\text{Si-Si}} = 520 \text{ cm}^{-1}$ , is observed, and it indicates to some unreacted silicon remaining. We showed earlier [15] that the phase composition of synthesized ceramics depends on the mass ratio of initial silicon and carbon matrix,  $\psi = \text{Si/C}$ . It can be concluded from the higher intensity of the Si–Si mode in the Raman spectra (Fig. 6) that the total volume of the unreacted silicon is larger in the case of impregnation with liquid silicon. The *D* and *G* bands related with the carbon matrix were not detected, which can be caused by additional annealing of the synthesized structures at 700 °C in air (spectra are not shown). The spectrum of

SiC synthesized by impregnation of carbon matrix with gaseous silicon (Fig. 6, curve 1) reveals the intense TO and weak unstructured LO bands. Analysis of the TO band shows that it is a superposition of TO modes 3C and 6H SiC polytypes. This is in agreement with our previous study [15], where bio-SiC formed from wood was shown to contain only 3C polytype for synthesis temperatures up to  $T_{\text{max}} \sim 1550 \text{ °C}$ , while for temperatures up to 1800 °C both 3C and 6H polytypes coexist.

As to the weak intensity of the LO bands, this fact is due to the different mechanisms of the Raman scattering by LO and TO phonons – the Frölich and deformation potential coupling mechanisms. In the work [16], the Raman scattering cross section,  $\sigma$ , was shown to depend on the excitation quanta energy,  $\hbar\omega$ , as  $\sigma \propto (E_g - \hbar\omega)^{-1}$  for deformation potential and as  $\sigma \propto (E_g - \hbar\omega)^{-3}$  for Frölich mechanism, with  $E_g$  being the band gap. It follows from the above relations that the scattering by LO phonons will weaken much faster with increasing the separation between the excitation energy and electronic transition in the structure, as compared to the scattering by TO phonons. Thus, the LO mode can be observed only under resonance or near-resonant excitation conditions. The predictions of the work [16] were supported experimentally in the works [17, 18] which studied the excitation wavelength dependence of the Raman scattering in SiC nanorods. On the other hand, the broad unstructured band between 800 and 950 cm<sup>-1</sup> in the spectra in Fig. 6 can be an indication of the SiC being partly in the amorphous phase.

The Raman spectrum of bio-SiC formed by impregnation of carbon matrix with liquid silicon (Fig. 6, curve 2) differs from that corresponding to impregnation with gaseous silicon. The TO band has one intense peak that corresponds to the contribution of 3C polytype dominating over that of the 6H. Thus, we conclude that under this synthesis conditions the portion of the 6H polytype is smaller than that in 3C. The presence of LO peak evidences a less amorphous phase in this sample.

It should be noted that for both SiC structures we observed a strong photoluminescence under excitation with 514.5 nm laser line. Further investigations are needed, however, in order to ascertain whether this luminescence is related with synthesized bio-SiC or with nanocrystalline Si in the pores of the structure.

#### 4. Conclusion

Biomorphic SiC ceramics produced by impregnation with liquid or vapor silicon of carbon matrices derived from peas (*Pisum sativum L.*) and beans (*Phaseolus*) precursors have been investigated. The structure and composition of the materials obtained were investigated using different techniques such as optical microscopy,

scanning electron microscopy, and Raman spectroscopy. It has been shown that the carbon matrix and consequently SiC ceramics made from endosperm has indeed inherited the alveolate structure and possesses many hierarchical pores with diameters varying from 20 up to 100  $\mu\text{m}$ . Raman spectroscopy investigations showed that the 3C polytype is formed at the synthesis temperature close to 1550  $^{\circ}\text{C}$ , and that both 3C and 6H-SiC are formed at temperatures up to 1800  $^{\circ}\text{C}$ .

#### References

1. Qing Wang, Guo-Qiang Jin, Dong-Hua Wang, Xiang-Yun Guo, Biomorphic porous silicon carbide prepared from carbonized millet // *Mater. Sci. and Eng. A*, **459**, p. 1-6 (2007).
2. A.R. Maddocks, A.T. Harris, Biotemplated synthesis of novel porous SiC // *Mater. Lett.*, **63**, p. 748-750 (2009).
3. Jingyun Huang, Xudong Wang, Zhong Lin Wang, Controlled replication of butterfly wings for achieving tunable photonic properties // *Nano Lett.*, **6**, N.6, p. 2325-2331 (2006).
4. Qing Wang, Donghua Wang, Guoqiang Jin, Yingyong Wang, Xiangyun Guo, Biomorphic SiC from lotus root // *Particuology*, **7**, p. 199-203 (2009).
5. M. Lopez-Alvarez, L. Rial, J.P. Borrajo, P. Gonzalez, J. Serra, E. Solla, B. Leon, J.M. Sanchez, J. Martinez Fernandez, A.R. de Arellano-Lopez, F.M. Varela-Feria, Marine precursors-based biomorphic SiC ceramics // *Mater. Sci. Forum*, **587-588**, p. 67-71 (2008).
6. P. Greil, Advance engineering ceramics // *Adv. Mater.* **14**, No.10, p. 709-716 (2002).
7. Jun-Min Qian, Zhi-Hao Jin, Xiao-Wen Wang, Porous SiC ceramics fabricated by reactive infiltration of gaseous silicon into charcoal // *Ceramics Intern.* **30**, p. 947-951 (2004).
8. O.P. Chakrabarti, H.S. Maiti, R. Majumdar, Biomimetic synthesis of cellular SiC based ceramics from plant precursor // *Bull. Mater. Sci.*, **27**, No.5, p. 467-470, October (2004).
9. L. Esposito, D. Sciti, A. Piancastelli, A. Bellosi, Microstructure and properties of porous b-SiC templated from soft woods // *J. Europ. Ceramic Soc.*, **24**, p. 533-540 (2004).
10. M. Presas, J.Y. Pastor, J. Llorca, A.R. de Arellano Lopez, J. Martinez Fernandez, R. E. Sepúlveda Ferrer, Microstructure and fracture properties of biomorphic SiC // *Intern. J. Refractory Metals and Hard Metals*, **24**(1-2), p. 49-54 (2005).
11. V.S. Kiselov, P.M. Lytvyn, V.O. Yukhymchuk, A.E. Belyaev, S.A. Vitusevich, Synthesis and properties of porous SiC ceramics // *J. Appl. Phys.*, **107**, 093510-6 (2010).
12. V.S. Kiselov, E.N. Kalabukhova, A.A. Sitnikov, P.M. Lytvyn, V.I. Poludin, V.O. Yukhymchuk, A.E. Belyaev, Effect of Si infiltration method on the properties of biomorphous SiC // *Semiconductor Physics, Quantum Electronics & Optoelectronics*, **12**(1), p. 68-71 (2009).
13. F. Tuinstra, J.L. Koenig, Raman spectrum of graphite // *J. Chem. Phys.* **53**, p. 1126-1134 (1970).
14. A.C. Ferrari, J. Robertson, Interpretation of Raman spectra of disordered and amorphous carbon // *Phys. Rev. B*, **61**, p. 14095-14107 (2000).
15. V.O. Yukhymchuk, V.S. Kiselov, A.E. Belyaev, M.Ya. Valakh, M.V. Chursanova, M. Danailov, S.A. Vitusevich, Raman spectroscopy of bio-SiC ceramics // *Phys. status solidi (a)*, **208**(4), p. 808-813 (2011).
16. R.M. Martin, Effect of electronic polarization on states of localized electrons in insulators // *Phys. Rev. B*, **4** (1971).
17. Y. Yan, Shu-Lin Zhang, S. Fan *et al.*, Effect of changing incident wavelength on Raman features of optical phonons in SiC nanorods and TaC nanowires // *Solid State Commun.*, **126**, p. 649-651 (2003).
18. Y. Ward, R.J. Young, R.A. Shatwell, Effect of excitation wavelength on the Raman scattering from optical phonons in silicon carbide monofilaments // *J. Appl. Phys.*, **102**, 023512 (2007).